Received: 28 May 2020 | Revised: 18 January 2021 | Accepted: 19 January 2021

IET Science, Measurement & Technology

DOI: 10.1049/smt2.12040

The Institution of Engineering and Technology WILEY

ORIGINAL RESEARCH PAPER

Numerical study of treatment chambers for single and multi-stage pulsed electric field systems

Eduardo J. Araujo[1,2] | **Ivan J. S. Lopes**[3] | **Jaime A. Ramirez**[3]

[1] Federal Institute of Minas Gerais, Campus Itabirito, St. José Benedito 139, Itabirito, Minas Gerais, Brazil

[2] Graduate Program in Electrical Engineering, Federal University of Minas Gerais, Belo Horizonte, Brazil

[3] Department of Electrical Engineering, Federal University of Minas Gerais, Belo Horizonte, Brazil

Correspondence:
Eduardo J. Araujo, Federal Institute of Minas Gerais, Campus Itabirito, St. José Benedito 139, 35455-040, Itabirito, Minas Gerais, Brazil.
Email: edu_jose0701@yahoo.com.br

Abstract

Pulsed electric field (PEF) systems should be designed to be microbiologically and energy efficient for industrial applications applied to treatment of different types of liquid foods. A thorough numerical model for the design of PEF systems is presented. It takes into account two combined approaches, a field evaluation based on an electric-thermal-fluid dynamic analysis and a design of numerical experiment considering as variables the applied high voltage and the internal electrode radius of a coaxial geometry. Then, the survival ratio and the specific energy are solved as conflicting objectives for the PEF design, using the treatment time and pulse frequency from the coupled analysis. The formulation is applied for grape and orange juices with *E. coli* for single and multiple stages systems. The simulations with multiple stages for the grape juice showed that it is possible to reach a microbial inactivation of 3.1 (log10 scale of survival rate) with a specific energy of about 450kJ/kg lower in relation to a two stage system. It means an energy reduction of 92, 421kJ/h for a treatment system with a capacity of 163 L/h.

1 | INTRODUCTION

Nowadays, there is a growing demand for high quality food products in relation to the nutritional and sensory characteristics. Considering that conventional heat treatment methods often affects the taste and nutritional value of foods, research on non-thermal technologies has developed considerably in recent decades. Among these technologies, pulsed electric field (PEF) has shown levels of inactivation of pathogenic microorganism of foods within the limits of consumer acceptance and is one of the most promising non-thermal techniques, which preserves the liquid foods by inactivation of microorganisms and also retains their nutritional and sensory attributes [1–3]. A typical PEF system consists of a high-voltage pulse generator, a treatment chamber, a fluid-handling system, control and monitoring devices [4]. For a short time (1–100 μs), the high voltage pulses are applied to the liquid placed between electrodes, generating an electric field on the liquid food product, which is responsible for the irreversible cell membrane breakdown in microorganisms leading to their elimination [5, 6].

The microbiological efficiency of a PEF system, represented by the microbial inactivation of the microorganism, is mainly dependent on the electric field distribution and the treatment time. Another parameter of interest in a PEF system is the specific energy, which measures the energy efficiency and is an important indicator that the system maintains its non-thermal characteristics, considering its relation with thermal dissipation of the liquid under treatment [7, 8]. Considering the electric field and the treatment time as variables, the microbial inactivation is higher as the specific energy increases and vice versa [9]. In this paper, the duality between these parameters is analysed from a computational point of view. The simultaneous analysis of these parameters allows the designer to adjust the design and process variables according to the specificities of each process with respect to microbiological and energy efficiency.

Numerical simulations of a high voltage pulse treatment system is an important stage of development that precedes the experiments and can provide temporal and spatial distribution of the electric field and temperature within the treatment chamber [10, 11]. In an earlier study presented by the authors [12], a computational model based on electric-thermal coupled analysis and multi-objective optimization was applied to a static coaxial treatment chamber. In the present study, the fluid dynamic analysis is incorporated in order to analyse the laminar flow

parameters. The addition of fluid dynamic analysis makes the computational model closer to a real system, considering the importance of synchronizing the frequency of the high voltage power supply with the transit time of the liquid inside the chamber. In addition, the calculation of the parameters related to the fluid flow are relevant to the specification of protocols for industrial PEF systems.

The methodology is applied to two case studies, considering different types of juices and systems with multiple stages. The simulations for different types of juices (grape and orange) with bacterium *E. coli* is used for comparison of the efficiency for treatment of liquids with different physicochemical properties. The different conductivities of these juices result in different limits of treatment times, considering the maximum temperature of 45 °C specified for this study, and impacts on the system efficiency. PEF experimental studies of liquids of different conductivities have been reported in the literature, such as in [13], in which the microbial inactivation of unpasteurized fruit juices of mango and papaya with different concentrations of *L. monocytogenes* was analysed, and in [14], in which a microbial inactivation and energy consumed for carrot juice containing bacteria *E. coli* was analysed in function of electric field and treatment time. The computational model applied to different liquids is an important tool to be used as a complement of experimental works, so that, from a coupled thermal-electric-fluid dynamic analysis, it is possible to analyse, computationally, the behaviour of the system efficiency as a function of the physicochemical characteristics of the liquid and other parameters of a PEF system, such as the applied voltage, the treatment time and the dimensions of the treatment chamber.

One of the main challenges in PEF treatment chamber design is the scalability of the chamber for industrial applications and one way to solve this problem is to use multiple treatment chambers [15]. In [16], an experimental work using four treatment chambers connected in series was carried out for the investigation of microbial inactivation of *E. coli* in milk for different concentrations, treatment times and electric field distributions. In the second case study presented in this paper, the computational model is applied in two and three-stage cascade systems in order to search for solutions with higher microbial levels, compared to a single stage system, and lowest energy consumption, respecting the thermal limits. It contributes to the design of PEF systems for industrial applications, considering that the proposed computational tool allows the designer to select specific levels of microbial inactivation and specific energy within a set of solutions for each stage of the system, properly setting the PEF parameters.

The paper is organised as follows: in the next section, the models and methods are discussed, with description of the dynamic treatment chamber, material properties, pulse characteristics, modelling of the microbial inactivation, governing equations of the physical processes and the computational modelling. In Section 3, the results are presented and discussed, including the results obtained directly from COMSOL and post processed results with the analysis of the two case studies. Finally, Section 4 summarizes and concludes the work.

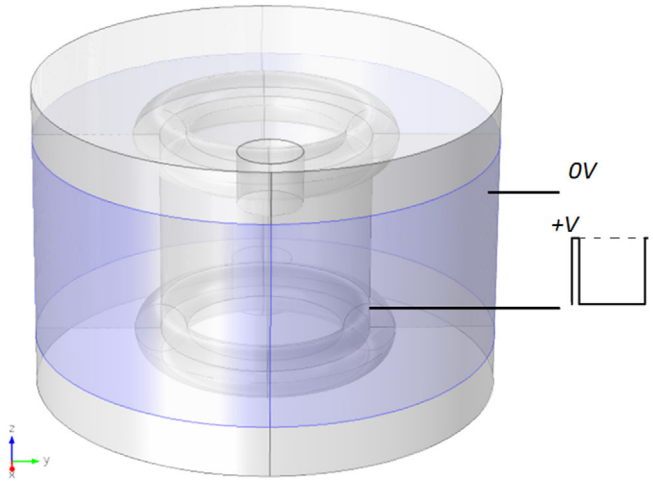

FIGURE 1 Coaxial treatment chamber

2 | MODELS AND METHODS

2.1 | Treatment chamber

The multiphysics simulations of this study are based on a coaxial treatment chamber reported in an earlier study presented by the authors [12], with the addition of liquid outlet for fluid flow. The coaxial chamber, indicated in Figure 1, has an effective liquid volume between 24 and 29 mL, which depends on the value of the internal electrode radius, ranging from 0.5 to 1.0 cm. The first case study of this work uses a single coaxial treatment chamber. In the second case study, coaxial treatment chambers are connected in cascade for the analysis of the microbial inactivation and specific energy.

2.2 | Material properties

The electrodes and top and bottom toroidal rings of the treatment chamber are made of stainless steel. The top and bottom insulators, which are made of PTFE (Teflon), are inserted in order to reduce the electric field strength. The properties of the materials used in the electrodes and insulators were obtained from COMSOL database and are available in the Appendix A.

The thermo-physical properties of juices vary depending on the temperature of the liquid. The specific heat, thermal conductivity and density also vary as a function of the dry matter value (X), which means the amount of material remaining after extracting all the liquid part. The viscosity of the liquid varies as a function of its Brix grade (B_x), which represents the amount of sucrose diluted in 100 g of the solution. The functions that represent the properties of juices are also available in the Appendix A.

The juices electrical conductivities were experimentally determined using a conductivity meter (CD-850 Conductivity meter, Instrutherm Ltd, São Paulo, Brazil) of commercially available juice samples (Maguary juice, produced in Araguari, Minas Gerais, Brazil). The data obtained as a function of temperature (20–50 °C) were adjusted by regression using

MatLabR2010 statistics toolbox. The electrical conductivity obtained for orange and grape juice are expressed in (1) and (2), respectively:

$$\sigma(T) = 8.7 \times 10^{-3} \cdot T + 1.658 \times 10^{-2} \mathrm{S/m}, \quad (1)$$

$$\sigma(T) = 3.5 \times 10^{-4} \cdot T + 8.875 \times 10^{-2} \times 10^{-2} \mathrm{S/m}, \quad (2)$$

where $\sigma(T)$ is the electrical conductivity dependent on temperature [S/m] and T is the temperature [°C].

2.3 | Pulse characteristics

A rectangular pulse waveform was used in the numerical simulations. It has the following features: peak value of 24 kV, width of 10 μs, a typical value for this application [17], rise and fall times of 2 μs, in order to avoid errors during processing and to approximate the specifications of real high voltage power supplies for PEF applications. According to [17], the dv/dt values in the rise and fall of the pulse have no significant influence on the treatment efficiency, since the time is much shorter than the pulse duration. The evaluation of the influence of the voltage pulse transient in the model, considering the model purely resistive circuit (R) and resistive/capacitive circuit (RC) is discussed in the Appendix B.

The pulse frequency was calculated as a function of the fluid flow time inside the treatment chamber, considering that the flow time must be synchronized with the pulse frequency, so that a given portion of the fluid receives all pulses from the high voltage power supply during fluid flow within the treatment zone.

2.4 | Modelling microbial inactivation

The development of mathematical models that estimate microbial inactivation of microorganisms as a function of system parameters is an important step in the design of a PEF treatment system, enabling equipment manufacturers to predict and control the safety and shelf life of food products at the system design stage [18].

The survival rate of microorganisms S is given by the ratio between the final number of microorganisms (N_f) and the initial number of microorganisms (N_i), according to equation,

$$S = \frac{N_f}{N_i}. \quad (3)$$

This study uses the Weibull model to estimate the microbial inactivation, considering its accurate results when compared to other models, such as the Hulsheger and Peleg models. The classical expression of the Weibull model is presented in the Equation (4) [19, 20]. It estimates the microbial inactivation using two parameters, called scalar parameter (δ) and shape parameter (β). The scalar parameter is the time at which microbial inactivation $\log_{10} S(t) = -1$, which represent a 90% reduction in the initial population of the microorganism under analysis. The β parameter represents the shape of the curve as follows: $\beta < 1$ corresponds to the upward concavity, $\beta > 1$ corresponds to the downward concavity and $\beta = 1$ to the linear curve,

TABLE 1 Parameters of the Weibull model to *E. coli* in grape and orange juices

***E. coli* (grape juice)**				
A_0	A_1	A_2	A_3	β_{av}
3.31	-3.68×10^{-2}	-1.08×10^{-3}	-9.45×10^{-7}	0.661
***E. coli* (orange juice)**				
A_0	A_1	A_2	A_3	β_{av}
1.64	$-1,50 \times 10^{-1}$	2.40×10^{-2}	–	0.274

$$\log S(t) = -\left(\frac{t}{\delta}\right)^{\beta}, \quad (4)$$

where S represents the survival rate and t is the treatment time.

The Weibull model can be expressed by tertiary models of microbial inactivation as a function of the electric field and treatment time,

$$\log_{10} S(t, E) = -\left[\frac{t}{10^{(A_0 + A_1 E + A_2 E^2 + A_3 E^3)}}\right]^{\beta_{av}}, \quad (5)$$

where A_0, A_1, A_2, A_3 are coefficients of the polynomial regression, t is the treatment time s, β_{av} is the average of the shape coefficient of Weibull model and E is the electric field strength [V m^{-1}].

The Weibull model can also be expressed in exponential form, as presented in [21],

$$S(t, E) = e^{\left(-\frac{t}{10^{(A_0 + A_1 E + A_2 E^2 + A_3 E^3)}}\right)^{\beta_{av}}}. \quad (6)$$

The parameters of the Weibull model for the bacterium *E. coli* in grape and orange juices were extracted from experimental studies reported in [22] and [23], respectively. The data for grape juice refer to (5) and the data for orange juice to (6) (exponential model). Table 1 summarizes the parameters of the Weibull model used in this study.

2.5 | Governing equations

2.5.1 | Electric field calculations

The governing equation for the electric potential is based on the charge conservation principle:

$$\nabla.(\sigma(T)\nabla V) = 0, \quad (7)$$

where $\sigma(T)$ is the electrical conductivity dependent on temperature [S m^{-1}] and V the electric potential [V].

Assuming no generation of electromagnetic forces, the relation between the electric field and the electric potential is described by:

$$E = -\nabla V, \tag{8}$$

where E is the electric field strength [V m^{-1}].

Dirichlet boundary conditions were set as zero for the grounded external electrode. The rectangular pulse, with initial voltage V, pulse width 10 μs and frequency 100 Hz, was set in the internal electrode and the rings.

2.5.2 | Temperature calculations

The energy balance for a pure conductive heat transfer in a liquid energy balance is given by

$$\rho C_p(T)\left(\frac{\partial T}{\partial t}\right) + \nabla[-k\cdot\nabla T] = Q, \tag{9}$$

where ρ denotes the density [kg m^{-3}], $C_p(T)$ is the specific heat capacity [m^{2}s^{-2}K^{-1}], T is the temperature [K], k is the thermal conductivity [W m^{-1}K^{-1}].

The heat source Q is due the dissipation of energy by ohmic heating effects as expressed by [10],

$$Q = \sigma(T)|E|^2, \tag{10}$$

where $\sigma(T)$ is the temperature dependent electrical conductivity [S m^{-1}] and E is the electric field strength [V m^{-1}].

The outer wall of the treatment chamber insulators was considered thermal insulated and the external electrode walls were set as conductive, applying a heat flux boundary condition as expressed in

$$n\cdot(-k\nabla T) = h\cdot(T_{ext} - T), \tag{11}$$

where n represents the normal direction to the boundary, T_{ext} is the room temperature [K] and h is the heat transfer coefficient [W m^{-2}K^{-1}].

2.5.3 | Liquid flow calculations

The numerical calculations of pressure and velocity fields are based on the differential equations of mass conservation and the linear momentum conservation, as presented in [24],

$$\frac{\partial \rho}{\partial t} + \nabla.(\rho v) = 0, \tag{12}$$

$$\rho\left(\frac{\partial v}{\partial t} + v.\nabla v\right) = -\nabla p + \mu\nabla^2 v + \rho f, \tag{13}$$

where ρ is the liquid density [kg m^{-3}], v is the fluid velocity [ms^{-1}], P is the pressure [Pa] and μ is the fluid viscosity [Pa s].

TABLE 2 Factors and respective levels of DOE matrix

		Level				
Variable	**Unit**	**−−**	**−**	**0**	**+**	**++**
V	kV	16	18	20	22	24
r_i	cm	0.5	0.625	0.75	0.875	1.0

The boundary conditions for liquid flow set in COMSOL are the velocity at the inlet orifice surface and the outlet pressure. Inlet velocity is set to liquid as a function of required flow and outlet pressure is set to 1 atm (ambient pressure).

2.6 | Computational modelling

The computational model used in this study is based on the model presented in [12]. Here, the fluid dynamics was also considered in the simulations using COMSOL. Three modules were coupled for simulations: AC/DC for electrostatics, heat transfer for temperature analysis and CFD for fluid dynamics analysis. After creating the coaxial geometry in COMSOL and setting all variables, the simulations were performed from a DOE (design of experiments) matrix.

2.6.1 | DOE matrix

The DOE matrix was created with the variables related to the electric field distribution (applied voltage (V) and internal electrode radius of coaxial geometry (r_i)) with their respective levels, consisting of a factorial design 2^5 (two variables with five levels for each one), resulting in 32 combinations. The model in COMSOL was solved for each variables combination of DOE matrix, returning with the electric field average, temperature and fluid flow parameters in the treatment chamber.

The lower limit is identified as −−, intermediate as 0 and upper as ++. The upper limits of (V) and (r_i) have been specified to limit the electric field in the liquid to 50 kV/cm in order to avoid dielectric breakdown. The lower limit of the applied voltage was specified as two thirds of the upper limit. Table 2 shows the variables and levels used in the DOE matrix.

2.6.2 | Post processing calculations

The electric field and temperature inside the treatment chamber were numerically obtained by weighted averages in order to have more accurate results, as expressed by (14) and (15), respectively. In these equations, the results of electric field and temperature for each element of the mesh from were weighted by element volume,

$$E_{w_{av}} = \frac{\sum_{i=1}^{nel} E_i.v_i}{v_l}, \tag{14}$$

$$T_{w_{av}} = \frac{\sum_{i=1}^{nel} T_i.v_i}{v_l}, \tag{15}$$

where E_i is the electric field strength in the each element i [V m^{-1}], T_i is the temperature value in the each element i [K], v_i is the volume of the element i [m^3], v_l is the liquid volume [m^3], nel is the total number of elements in the liquid, $E_{w_{av}}$ is the weighted average of the electric field strength [V m^{-1}] and $T_{w_{av}}$ is the weighted average temperature [K].

In order to ensure a laminar flow inside the treatment chamber, a maximum value of Reynolds number (R_e) of 1800 was defined for this study. The fluid average velocity was calculated by (16), which is based on the classical Reynolds equation [24]. For a same type of juice, the inlet velocity was set in order to reduce the Reynolds number as the hydraulic diameter increases (smaller values of the internal electrode radius),

$$v_m = \frac{R_e \mu D_H}{\rho}, \tag{16}$$

where v_m is the average fluid velocity [m/s], R_e is the Reynolds number, μ is the dynamic viscosity [Pa s], ρ is the fluid density [kg m^{-3}]and D_H is the hydraulic diameter [m].

The transit time of the liquid inside the treatment chamber was calculated by the ratio between the fluid mass, which is expressed in terms of the density and fluid volume, and the mass flow, which was obtained numerically by

$$t_t = \frac{\rho v_l}{Q_m}, \tag{17}$$

where t_t is the transit time [s], ρ is the fluid density [kg m^{-3}], v_l is the volume of liquid inside the treatment chamber[m^3] and Q_m is the mass flow [kg/s].

Considering that the transit time represents the duration of pulse train applied to the liquid, the period of each pulse is given by (18), that is, the ratio between the total application time of the pulse train and the maximum number of pulses. The frequency of the pulses (f_p) is given by the inverse of the period of each pulse, according to (19),

$$T_p = \frac{t_t}{n_m}, \tag{18}$$

$$f_p = \frac{1}{T_p}, \tag{19}$$

where T_p is the period of the applied pulse [s], t_t is the transit time[s], n_m is the maximum number of pulses and f_p is the pulse frequency [Hz].

2.6.3 | Nonlinear regression analysis of electric field

The electric field values of DOE matrix obtained by (14) were adjusted by nonlinear regression to obtain the average electric field equation as a function of the variables voltage and internal electrode radius. This adjustment was performed using the software Labfit, based on the classical electric field module equation

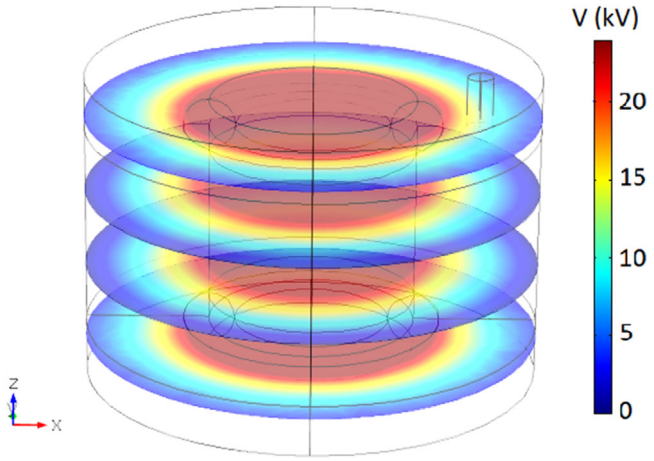

FIGURE 2 Potential distribution in the x–y planes in the treatment chamber for V = 24kV and r_i = 1 cm

for coaxial geometry given by:

$$E_r = k_1 \left(\frac{V}{\ln(r_e/r_i)} \right), \tag{20}$$

where E_r is the weighted average electric field obtained by nonlinear regression [V m^{-1}], k_1 is the coefficient, of adjustment, V is the applied voltage [V], r_e is the radius of external electrode [m] and r_i is the radius of the internal electrode [m].

The weighted electric field function (E_r) obtained by nonlinear regression adjustment was inserted in the microbial inactivation function, which is based on the Weibull model, (5) used for grape juice and (6) used for orange juice.

The specific energy (Q_s) in function n of the weighted electric field (E_r) is given by:

$$Q_s(t, E_r) = \frac{\sigma(T) E_r^{\,2} . v_l . t}{m}, \tag{21}$$

where Q_s is the specific energy [J/kg], E_r is the weighted average electric field obtained by nonlinear regression [V m^{-1}], t is the treatment time [s], $\sigma(T)$ is the temperature-dependent electrical conductivity [S m^{-1}] e m is the liquid mass [kg].

The microbial inactivation and specific energy functions represent the two conflicting objectives of the study and are associated with the specific restrictions of each case study investigated in this study.

3 | RESULTS AND DISCUSSION

3.1 | Electric field distribution

The electric field is calculated numerically by the finite element method from the potentials obtained in the mesh. Figure 2 shows cross sections of potential distribution in the effective chamber treatment region, considering an applied voltage of 24 kV and internal electrode radius of 1 cm. There is a symmetry

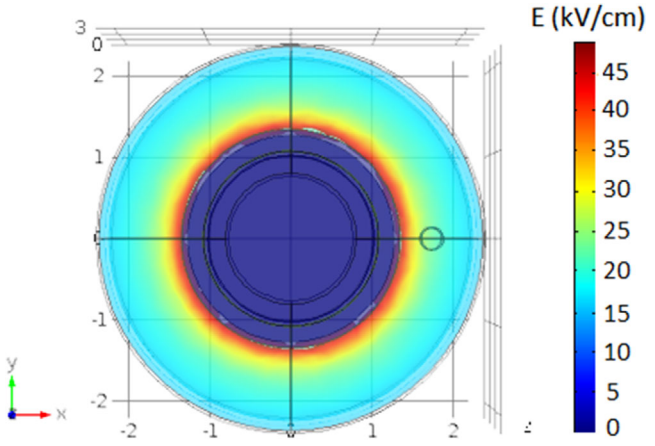

FIGURE 3 Top view of electric field at the top of the liquid treatment region for V = 24 kV and r_1 = 1 cm

in the distribution of potentials along the z plane of the chamber with a reduction of the values towards the external electrode.

A top view of the electric field distribution at the top of the liquid treatment region is shown in Figure 3 for the same configuration (V = 24 kV and r_1 = 1 cm), which represents the combination that generates a higher intensity electric field. Toroidal equalizers along with insulators were set within the treatment chamber to minimize the intensity of the electric field around the inner electrode edges. For this configuration, the electric field intensity is 48.2 kV/cm near the surface of the upper ring. The magnitude of the electric field is higher near the inner electrode surface and decreases toward the outer electrode surface, which is the expected behaviour for a coaxial geometry. A weighted average electric field of 21.4kV/cm was calculated using (14) for the condition analysed. The weighted average electric field values are used for numerical calculations of microbial inactivation and specific energy.

3.2 | Temperature

The liquid temperature plays an important role in the overall efficiency of the treatment considering that, as the temperature increases, the nutritional characteristics of the liquid may be affected. The temperature range of the liquid must be, preferably, in the range of 10 to 45 °C [25]. The application of PEF technology is restricted to low conductivity liquids, considering that an increase in liquid conductivity leads to an increase in the liquid's temperature during the application of pulses [26]. Figure 4 presents a comparison of temperature increase as function of a pulse application time for grape and orange juices, for V = 24 kV and r_1 = 1 cm. In this Figure, each temperature step corresponds to the application of pulse of 10 μs. The temperature for orange juice increases faster than grape juice, since orange juice has a conductivity about 3.7 to 4.8 times greater than the conductivity of grape juice in the temperature range of 20 to 45 °C. The maximum number of pulses for orange juice to reach the average temperature limit of 45 °C specified for the study is n = 5 pulses, which corresponds to a treatment time of

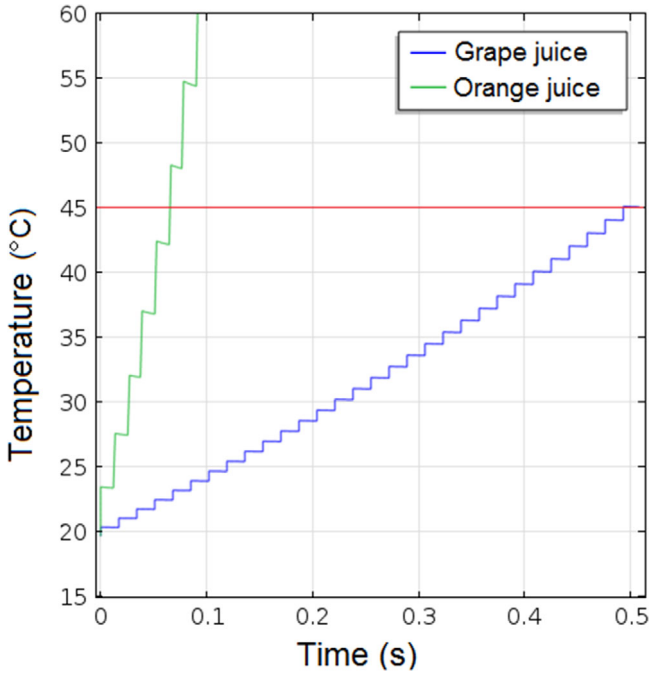

FIGURE 4 Average liquid temperature during application of pulses for grape and orange juices

50 μs. For grape juice n = 30 pulses, corresponding to a treatment time of 300μs. The higher conductivity of the orange juice does not contribute to microbial inactivation, since it limits the number of pulses, consequently, the treatment time. This analysis is relevant for defining the operation protocol of a PEF system for each type of liquid, considering that the number of pulses, and consequently the treatment time, must meet the system thermal limit.

3.3 | Fluid flow parameters

From the fluid dynamic analysis, it is possible to calculate the velocity of the fluid and synchronize with the pulse frequency in order to ensure that a given portion of the fluid receives all pulses from the high voltage power supply during fluid flow inside the treatment chamber. In this section, the results of velocity and pressure obtained from simulations in COMSOL using grape juice are discussed. Figure 5 presents a top view (cross section) of the fluid velocity distribution in the central region of the treatment chamber (z = 1.5 cm). The highest velocity of the liquid in the central plane of the treatment chamber (v = 0.59 m/s) occurs in the direction of liquid inlet port in the treatment chamber as reflection of the small turbulence generated when liquid is injected into the treatment chamber. Although this small reflection of the turbulence, the velocity of the liquid is homogeneous in most of the in the central region.

The liquid velocity as function of coordinate x from the inner electrode surface to a distance of 0.1 cm below the upper insulator is seen in Figure 6. The proximity to the liquid inlet leads to a non-uniform velocity in this region. The velocity reaches

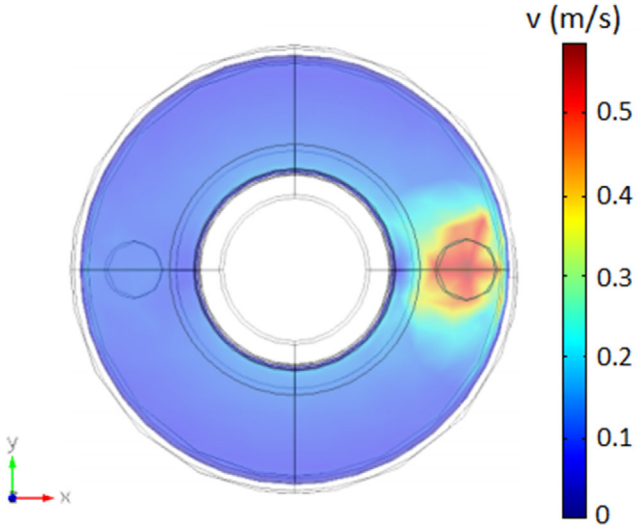

FIGURE 5 Top view (in section) of velocity distribution in central part of treatment chamber

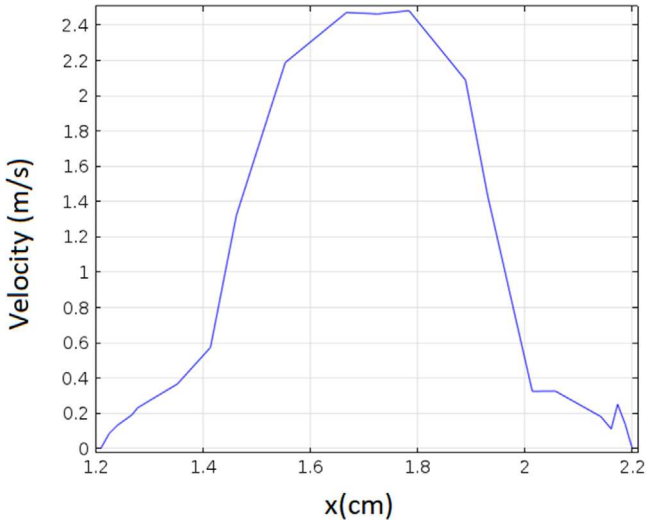

FIGURE 6 Velocity module as a function of coordinate x for 0.1 cm below top insulator

a maximum value of approximately 2.5 m/s near the inlet hole surface of the treatment chamber ($x = 1.7$ cm).

Although there are regions of non-uniformity of velocities, especially near the inlet and outlet of the liquid in the treatment chamber, in general, the velocity distribution in most of the treatment chamber can be considered homogeneous. Figure 7 shows the 3D distributions of velocity and pressure magnitude for grape juice. As showed, in most of the effective treatment region, both velocity and pressure have a homogeneous distribution, which is characteristic of laminar flow. The velocity magnitudes in the liquid inlet and outlet holes in the treatment chamber are larger due to the smaller cross-sectional areas, reaching a value of about 2.99 m/s in the liquid inlet region in the effective treatment region, due to the small zone of liquid turbulence in this region. The highest pressure value

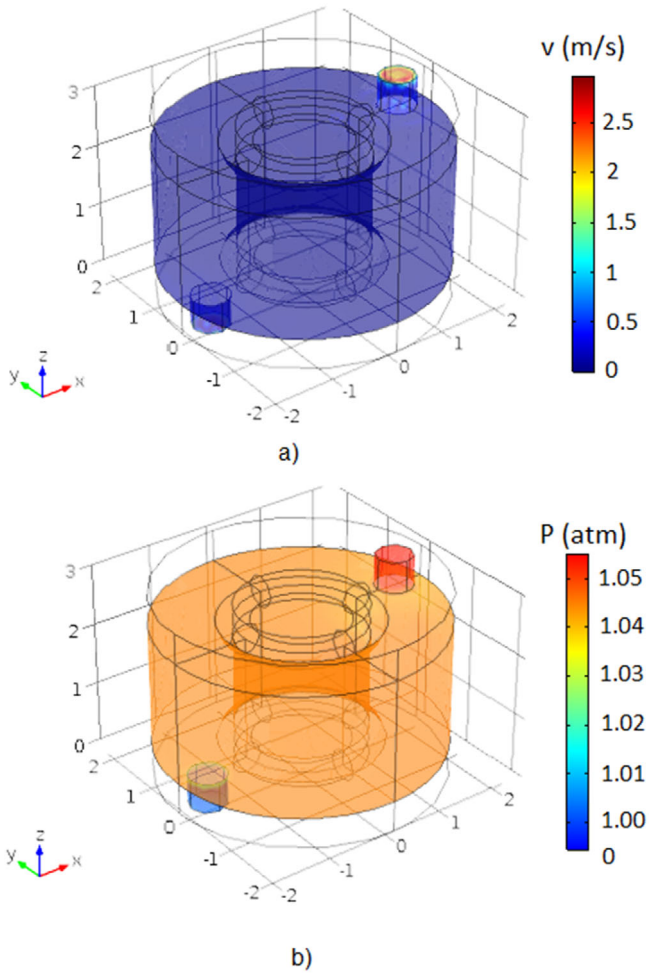

FIGURE 7 a) Velocity distribution b) Pressure distribution

(1.06 atm) occurs at the liquid inlet, for a boundary condition of 1 atm set at the liquid outlet.

For each type of juice analysed in this work, the average velocity of the liquid inside the treatment chamber for a laminar flow is used to determine the flow and pulse frequency of the high voltage power supply, as will be discussed in the Section 3.4.2.

3.4 | Post processed results

3.4.1 | DOE matrix and fitting

Table 3 presents the weighted average electric field results $E_{w_{av}}$ obtained for each combination of applied voltage values V and internal electrode radius r_i and the maximum electric field value E_{max} for each condition of the experimental matrix. The weighted electric field was obtained from (14), considering the electric field results in each element of the mesh weighting with the element volume. The electric field obtained ranged from 8.69 to 20.27 kV/cm and increases as the applied voltage and electrode radius increase, which is desirable for inactivation but impacts negatively on the energy efficiency of the system. It is emphasized that the electric field in the treatment region

TABLE 3 DOE matrix and electric field results

r_i(cm)	V(kV)	$E_{w_{av}}$ (kV/cm)	E_{max} (kV/cm)
0.5	16	8.69	28.2
0.625	16	9.68	28.3
0.75	16	10.79	29.9
0.875	16	12.05	30.2
1.0	16	13.51	32.4
0.5	18	9.78	31.8
0.625	18	10.90	31.9
0.75	18	12.14	33.6
0.875	18	13.56	34.0
1.0	18	15.20	36.4
0.5	20	10.87	35.3
0.625	20	12.11	35.3
0.75	20	13.49	37.3
0.875	20	15.07	37.7
1.0	20	16.89	40.3
0.5	22	11.95	38.7
0.625	22	13.32	38.8
0.75	22	14.84	40.5
0.875	22	16.58	41.4
1.0	22	18.58	44.3
0.5	24	13.04	42.2
0.625	24	14.53	42.3
0.75	24	16.19	44.6
0.875	24	18.08	45.0
1.0	24	20.27	48.2

is independent of the liquid conductivity as the impedance of the high voltage power supply is not considered in this study. The maximum electric field in the coaxial treatment chamber (48.2 kV/cm), obtained for the condition of $V = 24$ kV and $r_i = 1$cm, meets the limit of 50 kV/cm defined for this study.

The weighted electric field results were adjusted by nonlinear regression using (20) in Labfit software, resulting in a coefficient of $k_1 = 0.710$ for a coefficient of determination of $R^2 = 0.97$. Based on the ANOVA analysis of the variance test and adopting a significance level of 0.05, it was confirmed the effect of the factors r_i ($p < 2 \times 10^{-16}$), V ($p < 2 \times 10^{-16}$) and iteration between them ($p = 3.91 \times 10^{-8}$) on electric field values. From the k_1 value obtained, the average electric field obtained by nonlinear regression can be expressed by

$$E_r = 0.710\left(\frac{V}{\ln(2.2/r_i)}\right). \quad (22)$$

This expression of the weighted electric field is applied in the microbial inactivation and specific energy functions of the two case studies discussed in the next topic.

TABLE 4 Average values of dynamic viscosity and density for grape and orange juices

Parameter	Unit	Grape juice	Orange juice
μ_m	m Pa s	0.89	1.19
ρ_m	kg/m^3	1261	1103

TABLE 5 Results of flow parameters for grape and orange juices

Grape juice				
r_i(cm)	v_{in} (cm/s)	R_e	v_m (cm/s)	Q_m (kg/h)
0.5	225.1	1800	3.73	248.4
1.0	190.0	1268	3.73	205.2
Orange juice				
r_i (cm)	v_{in} (m/s)	R_e	v_m (cm/s)	Q_m (kg/h)
0.5	300.0	1800	5.71	295.2
1.0	260.1	1268	5.71	244.8

3.4.2 | Case study 1 - Comparing two different juices

in this case study, the fluid flow parameters for the two types of juices under study are initially calculated. Based on these results, the frequency of the high voltage power supply for each type of juice is obtained. Additionally, is presented a comparison of the Pareto curves for the juices, taking into account the two conflicting objectives, that is, microbial inactivation and specific energy.

Fluid flow

In order to calculate the average liquid velocity in the effective treatment region within the chamber for the two types of juices (grape and orange), the average dynamic viscosity (μ_m) and average density (ρ_m) were obtained for each type of juice, considering the minimum and maximum temperature values from the equations presented in the Appendix A. The average dynamic viscosity values were obtained for a Brix value B_x of 13 (typical value for non-concentrated juices), considering that one Brix means 1 g of sucrose per 100 g of solution. The average density of each juice was calculated for a juice dry matter value (X) of 30. Table 4 presents the results.

Table 5 summarizes the results of the flow parameters obtained for the 0.5 cm and 1.0 cm electrode radii for each type of juice, the average velocity (v_m) was calculated according to (16). For each electrode radius, the inlet velocity (v_{in}) was set in order to keep the same average velocity within the effective treatment region for each type of juice, resulting in the same pulse train frequency for the same type of juice. Then, from the average fluid velocity, the fluid mass flow (Q_m) was numerically calculated. Considering the same average velocity for each type of juice, the mass flow rate is larger for the radius 0.5 cm than for the radius 1 cm, as the hydraulic diameter is larger as the radius decreases. It is also observed that, for the same radius value of the internal electrode, the mass flow rate is higher for orange juice, due to the higher average velocity for this juice.

TABLE 6 Transit time, period and pulse rate results for each type of juice

Grape juice		
t_t (s)	T_p (s)	freq (Hz)
0.53	0.017	57.7
Orange juice		
t_t (s)	T_p (s)	freq (Hz)
0.39	0.013	76.9

From the mass flow results obtained for each type of juice electrode radius, (17), (18) and (19) were used to calculate transit time (t_t) of the liquid within the chamber, the period of each pulse (T_p) and the frequency of the pulses (f_p), respectively, which are presented in Table 6. These results indicate that the transit time and, consequently, the period of each pulse are shorter for orange juice. The same average velocity for the same type of juice for any internal electrode radius leads to the same transit time and frequency. Considering that orange juice flows faster through the effective treatment area in the chamber, due to its properties, the pulse frequency for this juice must be higher than for grape juice, in order to keep the transit time in accordance with the pulse frequency of the high voltage power supply. For the condition V= 24 kV, 300 μs and r_i = 1cm, the difference of average temperature in the liquid for the two frequencies was only 0.2 °C, which is not significant.

The transit time also defines the productivity of a PEF equipment for a particular type of liquid. As an example, considering the transit times obtained for the orange and grape juices for an internal electrode radius of 1 cm and a treatment volume of 24 mL, the system capacity would be 163 L/h and 221.5 L/h for grape and orange juices, respectively. Although the reduction of the transit time contributes to increased productivity, this may result in a Reynolds number higher than the limit for laminar flow as the velocity increases. In addition, as the system increases its capacity due to a reduction in transit time, it is necessary to verify that the frequency specification of the high voltage power supply meets to the required pulse frequency, considering that the frequency of the high voltage power supply should be increased as liquid flows faster through the treatment chamber.

Comparison of Pareto curves

The weighted electric field expression obtained by the regression (22) was inserted into the objective functions of microbial inactivation of the Weibull model (f_1) and specific energy (f_2). Considering the objective functions and constraints, including the different treatment time ranges for grape and orange juices due to the different conductivities, the formulation of the multiobjective optimization problem can be expressed by:

$$\min(f_1, f_2) \text{ subject to } \begin{cases} 16\text{kV} \le V \le 24\text{ kV} \\ 100\ \mu s \le t \le 300\ \mu\text{s (grape juice)} \\ 10\ \mu\text{s} \le t \le 50\ \mu\text{s (orange juice)} \\ 0.5\text{ cm} \le r_i \le 1\text{ cm} \end{cases} \quad (23)$$

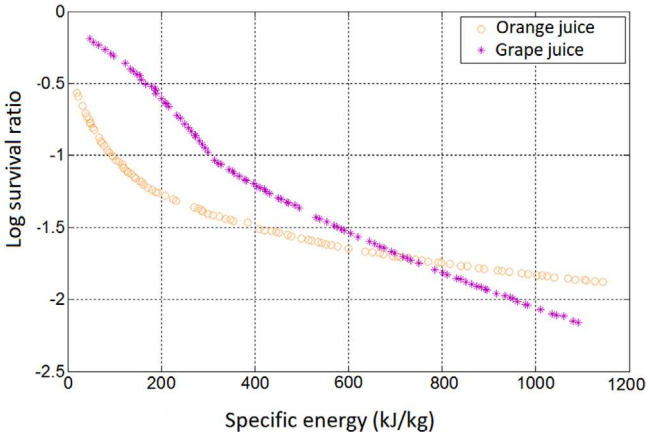

FIGURE 8 Pareto curves for different types of juice

Figure 8 presents a comparison of Pareto curves for both types of juice. The specific energy (X axis) represents the energy consumption per fluid mass and is related to the energy efficiency of a PEF process. Microbial inactivation (Y axis), in log of survival rate, express the relative number of living microorganisms that are eliminated by PEF treatment. As can be seen in the curve of both juices, an increase in microbial inactivation means an increase in the specific energy of the juice, that is, an increase in energy consumption. This compromise between microbial inactivation and specific energy is a crucial point in the design and setting of a PEF system. The points selected on each curve depend on the levels of the problem variables adjusted by the user for a specific process. Although the shorter treatment time for orange juice, due to the limitation of the number of pulses, better results are observed for this type of juice up to approximately the specific energy of 750 kJ/kg, that is higher microbial inactivation with lower energy consumption. This can be explained by the lower resistance of the bacterium *E. coli* in orange juice in relation to grape juice. From 750 kJ/kg, grape juice has better results of microbial inactivation, as the treatment time becomes dominant in relation to the resistance of the microorganism to treatment. These results show that the resistance of the microorganism to the PEF treatment and the conductivity of the liquid, which is related to the thermal limit and the treatment time, has a significant impact on the microbiological and energy efficiencies of the treatment, in addition to the electric field distribution.

A preview of the efficiency for different liquids allows the designer of a treatment chamber to analyse the behaviour of the system for different loads (liquids), checking if the design of a treatment chamber is compatible with the specifications of microbial inactivation and specific energy of a PEF system. In the case of a coaxial geometry, the designer can select 0.5 ≤ r_i ≤ 1 cm for a specific industrial application in which different types of juices will be processed. By adjusting the variables applied voltage and treatment time, which are part of the juice manufacturing protocol, it is possible to obtain the microbial inactivation and specific energy in the Pareto curves according to process requirements.

TABLE 7 Variables and objective functions values of selected points from the Pareto curves

		Variables			Objective functions	
Number	Juice	$V(kV)$	$t(us)$	$r_i(cm)$	f_1	$f_2(kJ/kg)$
1	*Grape*	24.0	220	1.0	−1.75	747.2
2	*Orange*	24.0	40	1.0	−1.74	744.9
3	*Grape*	16.7	120	0.7	−0.30	9.3
4	*Orange*	19.0	10	0.7	−0.80	49.8

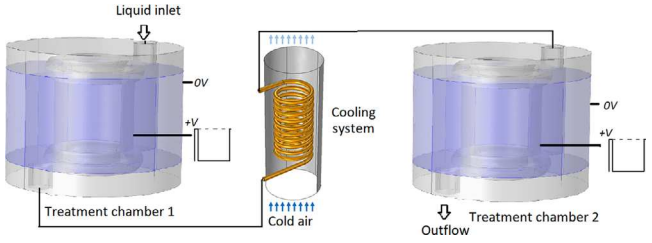

FIGURE 9 Two-stage treatment system

Table 7 shows the results extracted from the Pareto curves of the juices, including the variables related to each selected point. For example, for cases 1 and 2, a treatment chamber with the same value $r_i = 1$ cm could be selected to produce two types of juices with very close values of microbial inactivation and specific energy (intersection of Pareto curves), considering the adjustments in the applied voltage and treatment time, according to the values presented. In cases 3 and 4, another possible solution for a treatment chamber with an internal radius of $r_i = 0.7$ cm could be used to produce the juices with the values of applied voltage and treatment time presented. In these cases, although they are energy efficient operation points, microbial inactivations are relatively low for both juices, which directs the operation to applications in pre-treatment systems. Then, a treatment chamber with the same dimensions can be used for two different types of juice, through the appropriate selection in the Pareto curves, which adds in terms of cost and flexibility for the development of treatment chambers. In a real system, it must be set considering the specific values of the applied voltage and treatment time for each type of juice.

3.4.3 | Case study 2—Multi-stage systems

Depending on the requirements of the treatment process, it may be necessary to increase microbial inactivation. According to the Pareto curve obtained for the bacterium *E. coli* in grape juice, a microbial inactivation of −2.2 can be obtained for an specific energy of approximately 1100 kJ/kg. One of the options for increasing microbial inactivation, considering the restrictions of the problem in relation to the limits of the variables, is the connection of cascade treatment chambers, inserting a liquid cooling system between them, so that the liquid does not exceed the thermal limit of 45 °C specified for the study, as shown in Figure 9 for two stages of treatment.

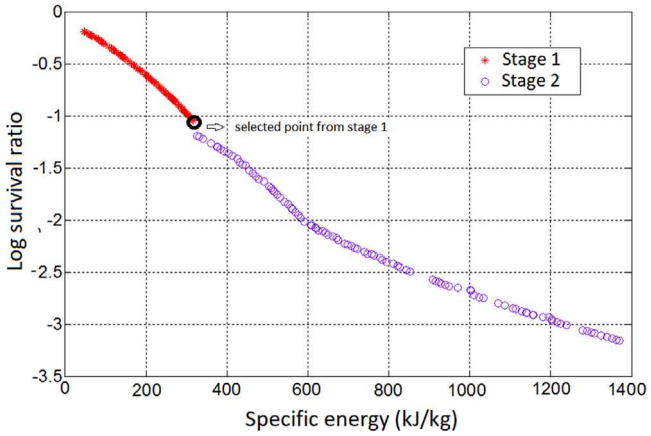

FIGURE 10 Pareto curves for two-stage cascade system

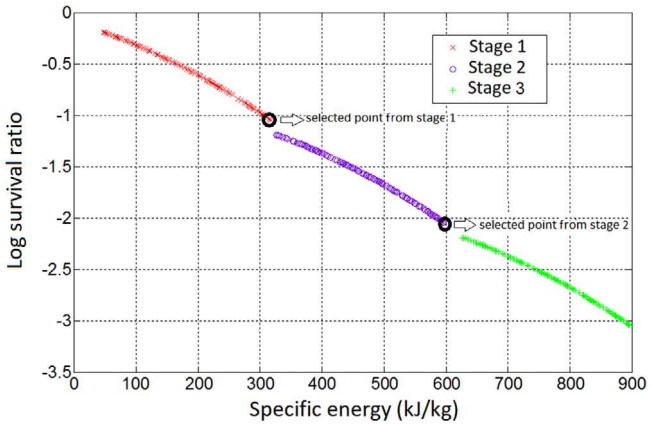

FIGURE 11 Pareto curves for cascade three-stage systems

The mathematical formulation of the multiobjective optimization problem for this study case, considering the inactivation of the bacterium *E. coli* in grape juice, is given by:

$$\min(f_1, f_2) \text{ subject to } \begin{cases} 16\text{kV} \le V \le 24\text{kV} \\ 100\ \mu\text{s} \le t \le 300\ \mu\text{s} \quad \text{(grape juice)} \\ 0.5\ \text{cm} \le r_i \le 1\ \text{cm} \end{cases} \tag{24}$$

Figure 10 shows the Pareto curves of a two-stage cascade system. A first stage (pre-treatment) can be implemented taking advantage of the region in which there is greater microbial inactivation with less specific energy, selecting the point of greatest microbial inactivation in this region. It refers to the saturation point of the electric field, with $V = 24$ kV, $r_i = 1$cm and $t = 100\ \mu$s, resulting in an inactivation of −1.1 for an specific energy of approximately 300 kJ/kg. The Pareto curve for the second stage shows the accumulated values of microbial inactivation and specific energy. As shown, the microbial inactivation value can reach −3.2 for an specific energy of approximately 1350 kJ/kg.

Figure 11 shows the Pareto curves for a three-stage system, considering the use only of the regions with greater microbial

inactivation with lower specific energies, that is, setting the treatment time for each stage at $t = 100\ \mu$s. By selecting the electric field saturation point with $V = 24$ kV and $r_i = 1$ cm in the first two stages, it is possible to achieve a microbial inactivation of up to −3.1 at the end of the third stage, which is very close to the microbial inactivation of the two-stage system, but with specific energy of 900 kJ/kg (33% lower). In this case, considering a system with capacity of 163 L/h for grape juice, as calculated from the frequency of the pulses (table 6), a reduction of energy of 92,421 kJ/h would be possible. Therefore, taking advantage of the region with the highest microbial inactivation, it is possible to obtain greater inactivation through the connection of more stages, with a lower specific energy.

The cost analysis for implementing cascade systems should be performed in order to evaluate the return on investment, considering the initial investment in the cascade system and the estimated energy savings for a specific microbial inactivation target.

4 | CONCLUSIONS

In this work, a thorough numerical model was applied in two case studies of orange and grape juices with *E. coli* in the analysis of single and multi-stage PEF systems.

The approach employed consists of an electric-thermal-fluidynamic field analysis combined with a design of numerical experiment. It takes into account the applied voltage and the internal electrode radius of a coaxial geometry and enables the user to calculate the maximum number of pulses and, consequently, the treatment time for each juice, in function of the thermal limit specified for the study. It is also possible to calculate the frequency of the pulses and transit time of the fluid inside the treatment chamber, important features for the PEF system design. In addition, the Pareto curve gives a trade off between survival ratio (inactivation) versus specific energy, which can be used appropriately.

The first case study, with a single stage system, indicates that the orange juice showed a higher microbial inactivation up to an specific energy of 750 KJ/kg due to the lower resistance to the treatment of the bacteria *E. coli* in this juice. From this point, the inactivation of grape juice becomes higher due the limitation of treatment time of orange juice. The second case study, with a multiple stage system, shows that with three-stage connection it is possible to reach microbial inactivation of about 3.1 (log10 of survival rate) with an specific energy of approximately 900 kJ/kg, i.e., 450 kJ/kg lower in relation to a two stage system. It means an energy reduction of 92,421 kJ/h for a grape juice treatment system with a capacity of 163 L/h.

The numerical model allows the designer of a treatment chamber of a PEF system to pre examine the behaviour of microbial inactivation and specific energy as a function of project and process parameters, selecting them accordingly. Based on the solution selected, the designer can develop single or multi-stage treatment chambers and define operation protocols, specifying the applied voltage and the number of pulses according to the required microbiological and energy efficiency of the liquid to be processed, which adds flexibility and efficiency in the development of PEF systems.

ACKNOWLEDGEMENTS

The authors thank the Brazilian agencies: CAPES, CNPq and FAPEMIG for the financial support provided to this study.

REFERENCES

1. Dziadek, K., et al.: Effect of pulsed electric field treatment on shelf life and nutritional value of apple juice. J. Food Sci. Technol. 56(3), 1184–1191 (2019)
2. Pal, M.: Pulsed electric field processing: an emerging technology for food preservation. J. Exp. Food Chem. 3(2), 2–3 (2017)
3. Gad, A., Jayaram, S.H.: Processing of carbonated beer by pulsed electric fields. IEEE Trans. Ind. Appl. 51(6), 4759–4765 (2015)
4. Nowosad, K., et al.: The application of PEF technology in food processing and human nutrition. J. Food Sci. Technol. 58(2), 397–411 (2020)
5. El-Hag, A.H., et al.: Survivability of inoculated versus naturally grown bacteria in apple juice under pulsed electric fields. IEEE Trans. Ind. Appl. 46(1), 9–15 (2009)
6. Zimmermann, U., Benz, R.: Dependence of the electrical breakdown voltage on the charging time invalonia utricularis. J. Membr. Biol. 53(1), 33–43 (1980)
7. Morales-de La-Peña, M., Elez-Martínez, P., Martín.Belloso, O.: Food preservation by pulsed electric fields: an engineering perspective. Food Eng. Rev. 3(2), 94–107 (2011)
8. Swami, S.S., et al.: Application of pulsed electric field in food processing. Int. J. Agric. Eng. 3(1), 171–174 (2010)
9. Mendes-Oliveira, G., Jin, T.Z., Campanella, O.H.: Modeling the inactivation of escherichia coli o157: H7 and salmonella typhimurium in juices by pulsed electric fields: The role of the energy density. J. Food Eng. 282, 110001 (2020)
10. Gerlach, D., et al.: Numerical simulations of pulsed electric fields for food preservation: a review. Innov. Food Sci. Emerg. Technol. 9(4), 408–417 (2008)
11. Ariza-Gracia, M.Á., et al.: Experimental and computational analysis of microbial inactivation in a solid by ohmic heating using pulsed electric fields. Innov. Food Sci. Emerg. Technol. 65, 102440 (2020)
12. Araujo, E.J., Lopes, I.J., Ramirez, J.A.: Computational modelling approach for the optimisation of a pulsed electric field system for liquid foods. IET Sci. Meas. Technol. 13(3), 337–345 (2018)
13. Rivas, A., et al.: Antimicrobial effect of stevia rebaudiana bertoni against listeria monocytogenes in a beverage processed by pulsed electric fields (pefs): combined effectiveness'. In: 1st World Congress on Electroporation and Pulsed Electric Fields in Biology, Medicine and Food & Environmental Technologies, pp. 43–46, Springer, Berlin (2016)
14. Singh, J., et al.: Sterilization of carrot juice with pulsed electric field treatment: A non-thermal preservation technique. In: Lynch, S. (ed.) Pulsed Electric Fields (PEF): Technology, Role in Food Science and Emerging Applications, pp. 115–128, Nova Science Publishers, Hauppauge, NY (2016)
15. El-Hag, A.H., et al.: A performance study of a multilevel electrode treatment chamber for food processing. IEEE Trans. Ind. Appl. 49(3), 1091–1097 (2013)
16. Alkhafaji, S.R., Farid, M.: An investigation on pulsed electric fields technology using new treatment chamber design. Innov. Food Sci. Emerg. Technol. 8(2), 205–212 (2007)
17. Loeffler, M.J.: Generation and application of high intensity pulsed electric fields. In: Raso, J., Heinz, V. (eds.) Pulsed Electric Fields Technology for the Food Industry, pp. 27–72, Springer, Boston, MA (2006)
18. Alvarez, I., et al.: Comparing predicting models for the escherichia coli inactivation by pulsed electric fields. Innov. Food Sci. Emerg. Technol. 4(2), 195–202 (2003)
19. Huang, K., et al.: A review of kinetic models for inactivating microorganisms and enzymes by pulsed electric field processing. J. Food Eng. 111(2), 191–207 (2012)

20. Cebrián, G., et al.: Resistance of escherichia coli grown at different temperatures to various environmental stresses. J. Appl. Microbiol. 105(1), 271–278 (2008)
21. Singh, J., et al.: Inactivation kinetic models for pulsed electric field treatment. In: Lynch, S. (ed) Pulsed Electric Fields (PEF): Technology, Role in Food Science and Emerging Applications. pp. 1–52, Nova Science Publisher, Hauppauge, NY (2016)
22. Huang, K., et al.: Comparing the pulsed electric field resistance of the microorganisms in grape juice: Application of the weibull model. Food Control 35(1), 241–251 (2014)
23. Rivas, A., et al.: Nature of the inactivation of escherichia coli suspended in an orange juice and milk beverage. Eur. Food Res. Technol. 223(4), 541–545 (2006)
24. Batchelor, G.K.: An Introduction to Fluid Dynamics. Cambridge University Press, Cambridge (2000)
25. Qin, B.L., et al.: Continuous flow electrical treatment of flowable food products. US Patent 5,776,529, 7 July 1998
26. Mohamed, M.E., Ayman, H., Eissa, A.: Pulsed Electric Fields for Food Processing Technology. IntechOpen, London (2012)
27. Simion, A., et al.: Modeling of the thermo-physical properties of grapes juice i. thermal conductivity and thermal diffusivity. Ann. Food Sci. Technol. 10(2), 363–368 (2009)
28. Simion, A.I., et al.: Modeling of the thermo-physical properties of grapes juice ii. boiling point and density. Scientific Study Res.Chem. Chem. Eng., Biotechnol., Food Ind. 10(4), 365–374 (2009)
29. Simion, A.I., et al.: Modeling of the thermo-physical properties of grapes juice iii. viscosity and heat capacity. Sci. Study Res.: Chem. Chem. Eng., Biotechnol., Food Ind. 12, 409–420 (2011)
30. Telis-Romero, J., et al.: Thermophysical properties of brazilian orange juice as affected by temperature and water content. J. Food Eng. 38(1), 27–40 (1998)
31. Zhu, X., Guo, W., Wu, X.: Frequency-and temperature-dependent dielectric properties of fruit juices associated with pasteurization by dielectric heating. J. Food Eng. 109(2), 258–266 (2012)

How to cite this article: Araujo EJ, Lopes IJS, Ramirez JA. Numerical study of treatment chambers for single and multi-stage pulsed electric field systems. *IET Sci Meas Technol.* 2021;15:385–397. https://doi.org/10.1049/smt2.12040

APPENDIX A

The properties of the materials used in the electrodes and insulators were obtained from the COMSOL database, as shown in Table A1.

In this paper, different types of juices (grape and orange) were used to evaluate the efficiency of the system. The physicochemical properties of juices depends on the liquid temperature. Specific heat, thermal conductivity and density also vary according to the dry matter (X), that is, the amount that remains of the mass of the material after extracting all the liquid. The liquid viscosity varies according to its Brix degree (B_x), which represents the amount of sucrose diluted in 100 g of the solution. The expressions of the properties of juices were extracted from literature studies, as shown in Table B1.

TABLE A1 Properties of materials used in electrodes and insulators

Stainless steel (electrodes)		
Parameter	**Unit**	**Value**
Thermal conductivity (k)	W/m K	44.5
Thermal capacity (C_p)	J/kg K	475
Density (ρ)	kg/m^3	7850
Teflon (insulators)		
Parameter	**Unit**	**Value**
Thermal conductivity (k)	W/m K	0.24
Thermal capacity(C_p)	J/kg K	2200
Density (ρ)	kg/m^3	1050

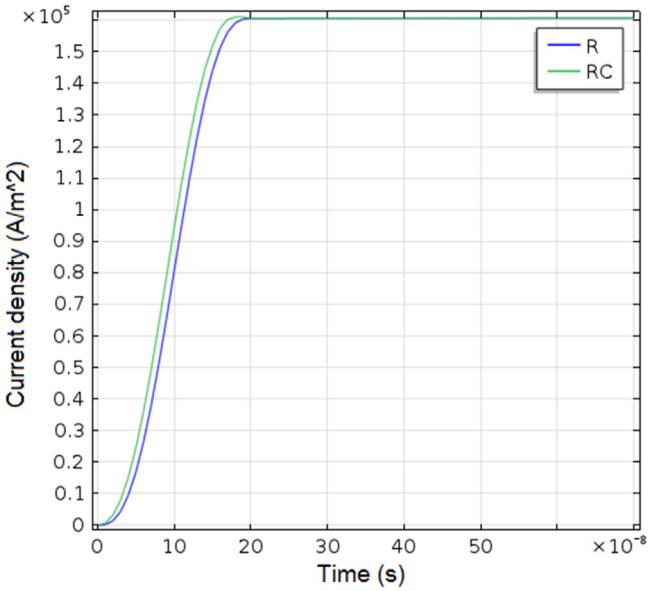

FIGURE B1 Current density for R and RC

APPENDIX B

The analysis of the effect of the voltage pulse transient in the model is based on the current density (J) during the voltage pulse rise time. Figure B1 shows the current density for two cases: purely resistive circuit (R) and resistive/capacitive circuit (RC), considering a relative permittivity of grape juice of 80 [31]. As shown, the current density waveform is not significantly affected by the capacitor, which means that the model is predominantly resistive for the considered pulse characteristics.

TABLE B1 Equations of the physicochemical properties of grape and orange juices

Grape juice

Parameter	Unit	Equation	Ref.
Thermal conductivity (k)	W/m K	$[0.565 + 1.8 \times 10^{-3}(T - 273) - 6 \times 10^{-6}(T - 273)^2](1 - 5.4 \times 10^{-2}X)$	[27]
Thermal capacity (C_p)	J/kg K	$1386 + 21.6(100 - X) + 2T$	[28]
Density (ρ)	kg/m^3	$1768 - 7(100 - X) - 0.928(T - 273) + 0.006(100 - X)(T - 273)$	[29]
Viscosity (μ)	m Pa s	$e^{-4.7989+4.63824\times10^5 T^{-2}+1.98\times10^{-4} B_x^2 lnB_x}$	[28]

Orange juice

Parameter	Unit	Equation	Ref.
Thermal conductivity (k)	W/m K	$0.079 + 0.523(100 - X) + 5.8 \times 10^{-5}(T - 273)$	[30]
Thermal capacity (C_p)	J/kg K	$1424 + 26.7(100 - X) + 2.45(T - 273)$	[30]
Density(ρ)	kg/m^3	$1428.5 - 4.549(100 - X) - 0.231(T - 273)$	[30]
Viscosity (μ)	m Pa s	$1.03 \times 10^{-4}(-4 \times 10^{-5} B_x^2 + 8 \times 10^{-5} B_x + 1.02)^{-19.9} e^{3.065\times10^3 T^{-1}}$	[30]